SUPPORTING INFORMATION

NLDFT Pore Size Distribution in Amorphous Microporous Materials

Grit Kupgan[†], Thilanga P. Liyana-Arachchi[‡], Coray M. Colina*[,†,‡]

[†]Department of Materials Science and Engineering and [‡]Department of Chemistry, University of Florida, Gainesville, 32611, United States

SIMULATED STRUCTURES

The majority of materials presented in this study were synthesized *in silico* using *Polymatic*[1,2] (except for OMIMs) followed by a compression/decompression scheme[3] for obtaining final structures. The force field abbreviation are as following: TraPPE-UA = Transferable Potentials for Phase Equilibria United Atom,[4–6] GAFF = Generalized Amber Force Field,[7] and PCFF = Polymer Consistent Force Field.[8]

Table S1 - Summary of microporous materials used in this work.

Name	**Description**	**Composition**	**Number of monomers**	**Box length**	**Non-bonded force field**	**Bonded force field**
PIM-1	Polymer of intrinsic microporosity[9]	100% PIM-1	100 PIM-1 monomers	43.5 ± 0.2 Å	TraPPE-UA	GAFF
HCP1	Hypercrosslinked polymer[10] - Poly(vinylbenzyl chloride-*co*-divinylbenzene)	98% vinylbenzyl chloride (VBC), 2% divinylbenzene (DVB)	196 VBC monomers, 4 DVB monomers	37.4 ± 0.3 Å	TraPPE-UA	PCFF
HCP2	Hypercrosslinked polymer[11] - Poly(styrene-*co*-vinylbenzyl chloride)	25% styrene (STR), 75% vinylbenzyl chloride (VBC)	50 STR monomers, 150 VBC monomers	37.1 ± 0.5 Å	TraPPE-UA	PCFF
HCP3	Hypercrosslinked polymer[11] - Poly(vinylbenzyl chloride)	100% vinylbenzyl chloride (VBC)	200 VBC monomers	37.8 ± 0.3 Å	TraPPE-UA	PCFF
PY1	Conjugated microporous polymer[12]	100% 1,3,6,8-tetrabromopyrene (A_4)	200 A_4 monomers	55.6 ± 0.4 Å	TraPPE-UA	PCFF
PY2	Conjugated microporous polymer[12]	75% 1,3,6,8-tetrabromopyrene (A_4), 25% 1,3-dibromo-7-*tert*-butylpyrene (B_2)	150 A_4 monomers, 50 B_2 monomers	43.1 ± 0.8 Å	TraPPE-UA	PCFF
OS-DVB1	0% crosslinked polyolefin[13]	81% octene, 19% styrene	162 octene monomers, 38 styrene monomers	35.5 ± 0.1 Å	PCFF	PCFF

Table S1 - Summary of microporous materials used in this work. (Continued)

Name	**Description**	**Composition**	**Number of monomers**	**Box length**	**Non-bonded force field**	**Bonded force field**
OS-DVB2	100% crosslinked polyolefin[13]	4.6% styrene, 95.4% crosslinked unit	9 styrene monomer, 191 crosslinked unit	35.3 ± 0.2 Å	PCFF	PCFF
DCX	Microporous polymer network[14] - Poly(dichloroxylene)	100% dichloroxylene	176 dichloroxylene monomers	32.4 ± 0.3 Å	PCFF	PCFF
OMIM1	Organic molecules of intrinsic microporosity with 1,4 fragments[15]	100% OMIM 1+4	100 OMIM 1+4 monomers	61.0 ± 0.2 Å	PCFF	PCFF
OMIM2	Organic molecules of intrinsic microporosity with 4,8 fragments[15]	100% OMIM 4+8	100 OMIM 4+8 monomers	75.9 ± 0.7 Å	PCFF	PCFF

Table S2 - Regularization parameter used in this work.

Name	**λ for NLDFT**	**λ for SSNLDFT**
PIM-1	1.00	5.00
HCP1	0.75	4.50
HCP2	0.75	4.50
HCP3	1.00	4.50
PY1	0.75	5.25
PY2	0.25	5.00
OS-DVB1	0.75	5.25
OS-DVB2	0.00	4.75
DCX	0.25	4.75
OMIM1	0.00	4.50
OMIM2	0.25	4.50

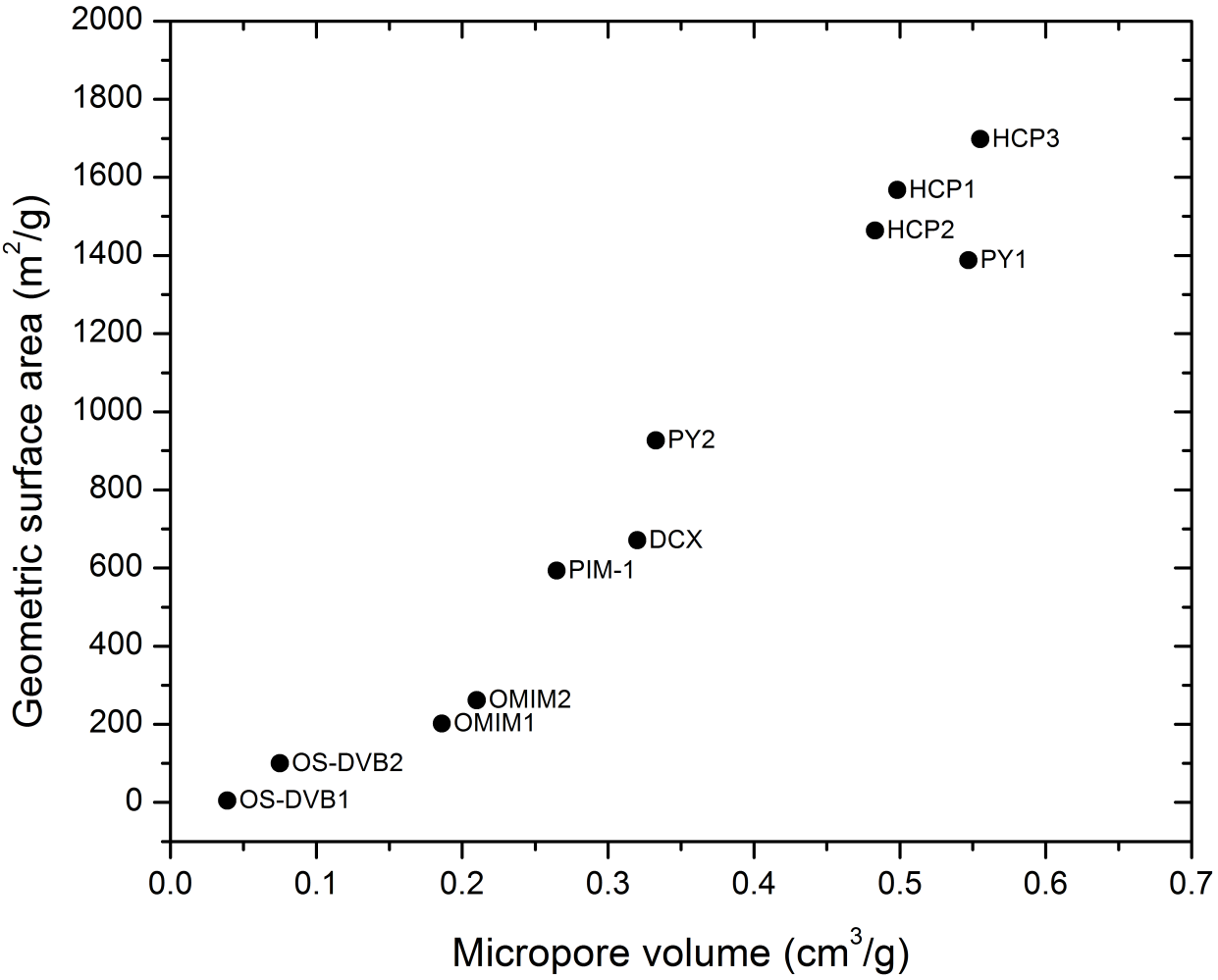

Figure S1 - The range of geometric surface area and micropore volume of amorphous materials investigated in this study.

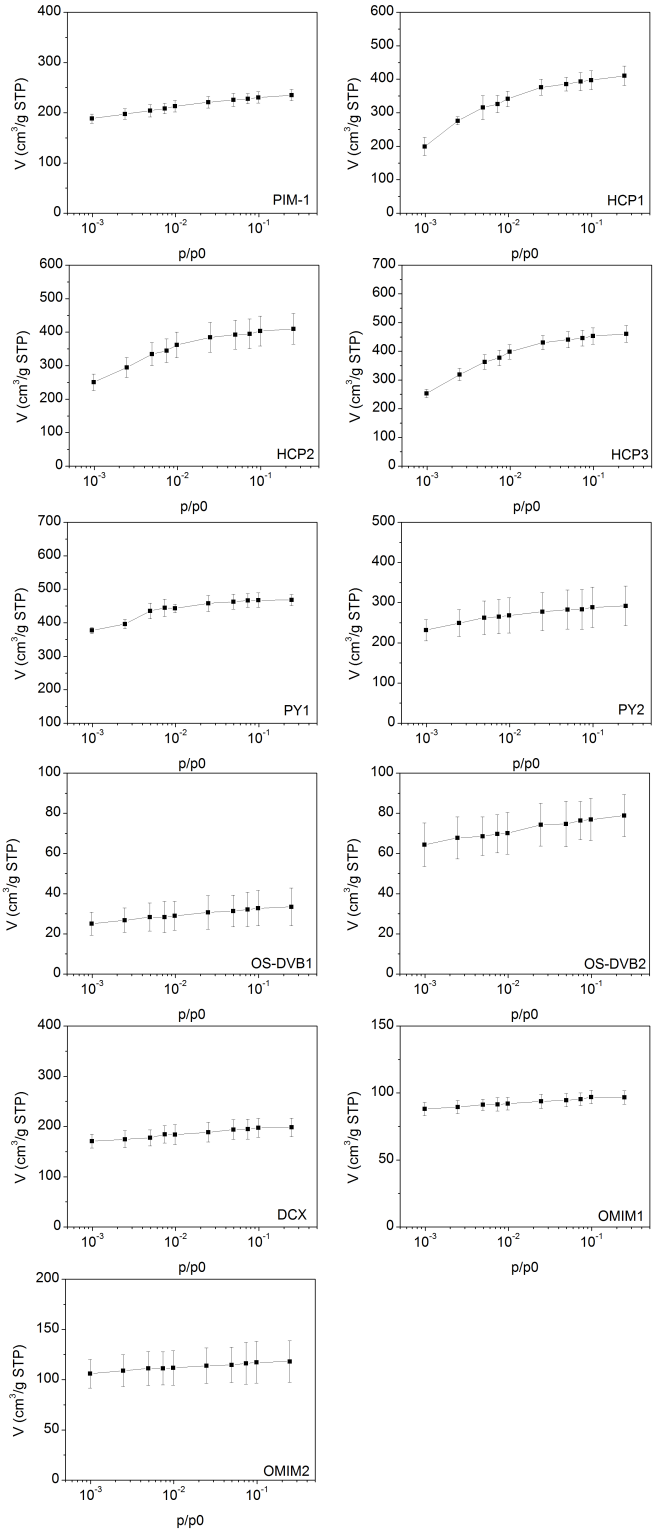

Figure S2 - N_2 adsorption isotherms at 77 K obtained from isobaric-isothermal Gibbs ensemble Monte Carlo (NPT-GEMC) simulations.

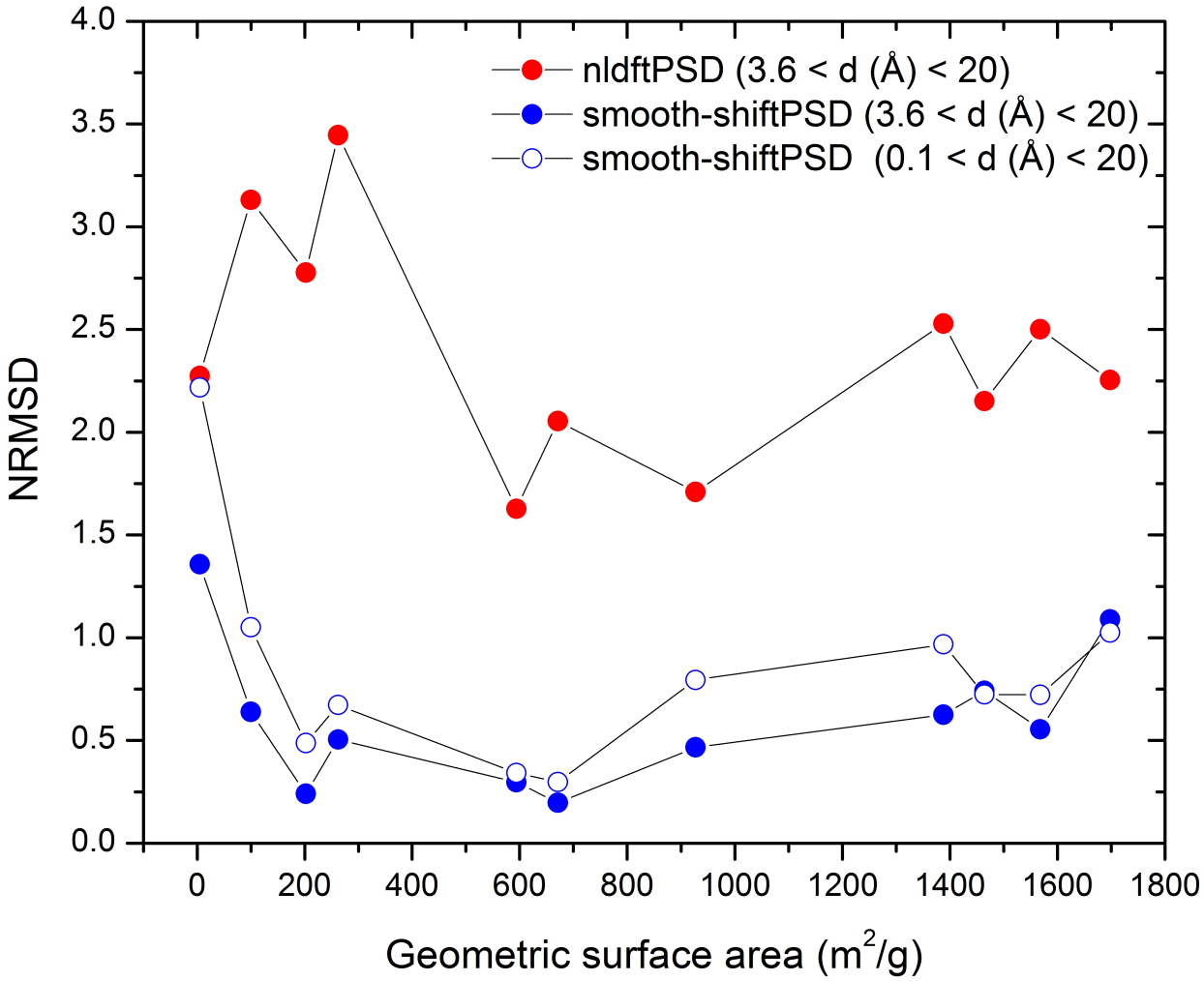

Figure S3 - Normalized root-mean-square deviation (NRMSD) as a function of the geometric surface area. NRMSD measured the deviation from the exact geometric pore size distribution. NRMSD was normalized by the mean of geometric PSD specifically for each material (Eq. S1).

$$NRMSD = \frac{RMSD}{\bar{y}} = \frac{\sqrt{\frac{\sum\left(PSD_i - PSD_{geo,i}\right)^2}{n}}}{\overline{PSD_{geo}}} \qquad \text{(Eq. S1)}$$

In this equation, RMSD is defined by summation of the difference squared between PSD of either NLDFT or smooth-shift and geometric PSD at the same diameter. The mean value of geometric PSD, $\overline{PSD_{geo}}$, is chosen as the mean value of measurement, $\bar{y}$, which normalizes RMSD. The normalization is required in order to compare materials with different PSD scales. The analysis includes evenly spaced 100 data points (n=100) using the range (d) indicated in Figure S3.

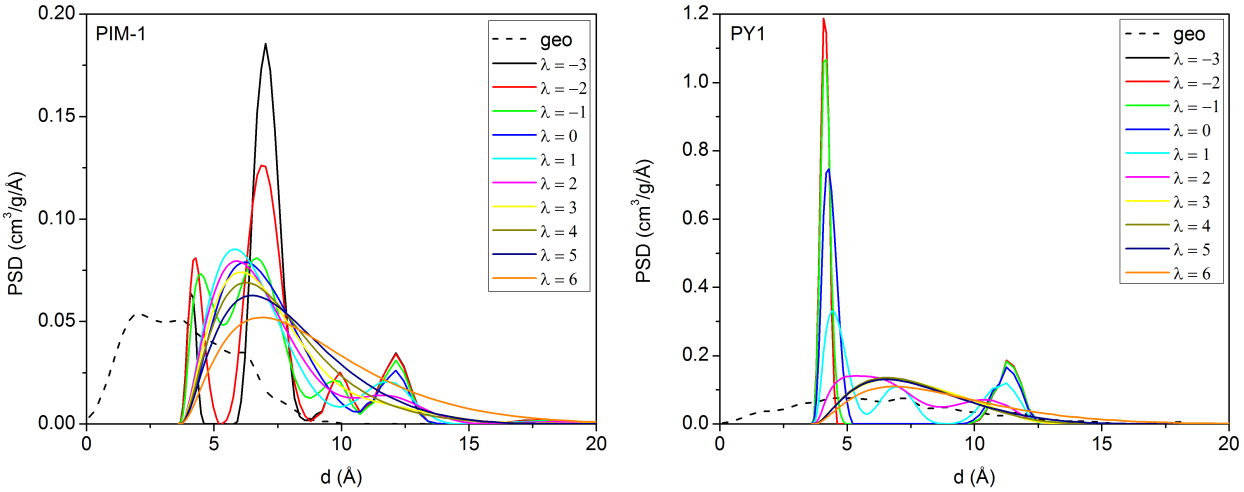

Figure S4 - NLDFT PSDs for PIM-1 (left) and PY1 (right) as a function of the regularization parameter, λ.

REFERENCE

(1) Abbott, L. J.; Hart, K. E.; Colina, C. M. Polymatic: A Generalized Simulated Polymerization Algorithm for Amorphous Polymers. *Theor. Chem. Acc.* **2013**, *132*, 1–19.

(2) Abbott, L. J.; Colina, C. M. Polymatic: A Simulated Polymerization Algorithm https://nanohub.org/resources/17278.

(3) Larsen, G. S.; Lin, P.; Hart, K. E.; Colina, C. M. Molecular Simulations of PIM-1-like Polymers of Intrinsic Microporosity. *Macromolecules* **2011**, *44* (17), 6944–6951.

(4) Martin, M. G.; Siepmann, J. I. Transferable Potentials for Phase Equilibria. 1. United-Atom Description of N -Alkanes. *J. Phys. Chem. B* **1998**, *102*, 2569–2577.

(5) Martin, M. G.; Siepmann, J. I. Novel Configurational-Bias Monte Carlo Method for Branched Molecules. Transferable Potentials for Phase Equilibria. 2. United-Atom Description of Branched Alkanes. *J. Phys. Chem. B* **1999**, *103*, 4508–4517.

(6) Wick, C. D.; Martin, M. G.; Siepmann, J. I. Transferable Potentials for Phase Equilibria. 4. United-Atom Description of Linear and Branched Alkenes and Alkylbenzenes. *J. Phys. Chem. B* **2000**, *104*, 8008–8016.

(7) Wang, J.; Wolf, R. M.; Caldwell, J. W.; Kollman, P. A.; Case, D. A. Development and Testing of a General Amber Force Field. *J. Comput. Chem.* **2004**, *25* (9), 1157–1174.

(8) Sun, H. Force Field for Computation of Conformational Energies, Structures, and Vibrational Frequencies of Aromatic Polyesters. *J. Comput. Chem.* **1994**, *15* (7), 752–768.

(9) Hart, K. E.; Abbott, L. J.; McKeown, N. B.; Colina, C. M. Toward Effective CO_2/CH_4 Separations by Sulfur-Containing PIMs via Predictive Molecular Simulations. *Macromolecules* **2013**, *46* (13), 5371–5380.

(10) Kupgan, G.; Liyana-Arachchi, T. P.; Colina, C. M. Pore Size Tuning of Poly(styrene-Co-Vinylbenzyl Chloride-Co-Divinylbenzene) Hypercrosslinked Polymers: Insights from Molecular Simulations. *Polymer* **2016**, *99*, 173–184.

(11) Abbott, L. J.; Colina, C. M. Formation of Microporosity in Hyper-Cross-Linked Polymers. *Macromolecules* **2014**, *47* (15), 5409–5415.

(12) Abbott, L. J.; Colina, C. M. Porosity and Ring Formation in Conjugated Microporous Polymers. *J. Chem. Eng. Data* **2014**, *59* (10), 3177–3182.

(13) Abbott, L. J.; Hughes, J. E.; Colina, C. M. Virtual Synthesis of Thermally Cross-Linked Copolymers from a Novel Implementation of Polymatic. *J. Phys. Chem. B* **2014**, *118* (7),

1916–1924.

(14) Abbott, L. J.; Colina, C. M. Atomistic Structure Generation and Gas Adsorption Simulations of Microporous Polymer Networks. *Macromolecules* **2011**, *44* (11), 4511–4519.

(15) Abbott, L. J.; McKeown, N. B.; Colina, C. M. Design Principles for Microporous Organic Solids from Predictive Computational Screening. *J. Mater. Chem. A* **2013**, *1* (38), 11950–11960.